

# Synthesis of Bimetallic Silver and Copper Alloy Nanoparticles Embedded with Styrene-Methyl Methacrylate Copolymer Nanosphere (SMMA@Ag-Cu) as a Potential Surface Enhanced Raman Scattering (SERS) Substrate

Wan Ahmad Lutfil Hadi Wan Abdul Halim<sup>1</sup>, Nor Shafeera Rasyada Shaiful Bahri<sup>1</sup>, Nur Aida Mohamed Shaul Hamid<sup>1</sup> and Syara Kassim<sup>1,2\*</sup>

<sup>1</sup>Faculty of Science and Marine Environment, Universiti Malaysia Terengganu, 21030 Kuala Nerus Terengganu, Malaysia

<sup>2</sup>Advanced Nano Materials (AnoMa) Research Group, Nano Research Team, Faculty of Science and Marine Environment, Universiti Malaysia Terengganu, 21030 Kuala Nerus, Terengganu, Malaysia

\*Corresponding author (e-mail: syara.kassim@umt.edu.my)

Photonic crystals (PCs) have great photon interaction with their periodic structure to create fascinating optical properties. Furthermore, when incorporating PCs with Ag-Cu alloy nanoparticles (NPs) in a core-shell structures it has unique linear optical properties that give great enhancements in electromagnetic field in the form of 3D- metallodielectric photonic crystals (MDPCs). However, silver and copper alloy NPs are not widely studied due to their unique localised surface plasmonic resonance (LSPR). Copper alone has a low stability and high tendency to oxidise, thus, silver was used to stabilise the interaction. In this research, combining both LSPR of Ag-Cu NPs and photonic resonance of PCs can create a substrate with high sensitivity towards light. By taking the approach of green sustainability, surfactant free-emulsion copolymerisation reaction was conducted. Copolymer was synthesised in the absence of emulsifiers and toxic solvent, while Ag-Cu NPs obtained from reduction of sodium borohydride. A polyethylene imine (PEI) linker was used to correlate between alloy NPs and copolymers. The UV-vis analysis showed the resulted core shell structure that provided spectrum with a sharp peak at 291 nm and under transmittance electron microscope (TEM) analysis, alloy NPs was strongly held on the spherical ball of copolymer with diameter of 450 nm indicating the successfulness combination of these two materials. In short, this synthesised substrate gave high potential and possibilities to be used as a substrate in surfaced enhanced Raman scattering (SERS).

**Keywords:** Photonic Crystals; metallo-dielectric; SMMA@Ag-Cu; core shell; Surface Enhanced Raman Scattering

*Received: January 2023 ; Accepted: February 2023*

Photonic crystal (PC) is an intriguing substance due to its unique optical characteristics and ability to be created synthetically. A characteristic of PC that results from its periodic arrangements is the photonic bandgap, which may be tailored to fit the needs of certain applications [1]. The PCs might be useful in a variety of applications, including polarisers, laser waveguides, photovoltaics, and biomedical engineering [2]-[4]. Since its development, it has been incorporated into a wide range of designs, including inverted, metallodielectric, fibres, and annular [5]-[7]. In this context, due to its combination of PCs with surface plasmon resonance, metallodielectric PCs (MDPC), a PC containing metal nanoparticles in either core-shell or wafer template structure, has become a captivating choice for sensor, detection, and surface-enhanced Raman scattering (SERS) investigation [8]. Formerly, basic material used to create PCs was silica but in the preparation of nanometre particle sizes, the use of

silica contributed massive toxicity towards the environment [9]. Therefore, choosing the right material is the most vital part to encounter this issue. In this research, styrene and methyl methacrylate (SMMA) copolymer were chosen as a basic material to create fully functional PCs due to their low cost and easy processing materials, while the use of bimetallic alloy nanoparticles created perfect light-gathering components for PCs [10].

Metals such as gold (Au), silver (Ag), and copper (Cu) have been widely investigated as the substrate source in the field of SERS due to the visible range localised surface plasmon resonance (LSPR) and surface plasmon polarisation (SPP) properties of free electrons in coinage [11]. However, Cu and Ag nanoparticles alone are not stable since Cu may quickly oxidise to create CuO and Cu<sub>2</sub>O, whereby Ag has problems with aggregations and low chemical stability

which poses a constraint for SERS experiments [12]-[14]. In order to overcome these limitations, by alloying Ag and Cu would allow the performance of two distinct metals combine into bimetallic nanoparticles [15]-[19]. For instance, prior investigations have suggested that Ag-Cu alloy plasmonic substrates have great strength, antibacterial activity, and reproducibility, whereas Ag-Cu core-shell plasmonic substrates have outstanding thermal stability, antioxidation and chemical stability [23]-[25]. Therefore, alloy Ag-Cu bimetallic nanoparticles are directly improving each metal chemical characteristic and hold promise in a variety of application fields, especially in SERS.

In this research, the green chemistry approach was employed since methods that reduce the usage of dangerous substances had been established. The PCs were synthesised via surfactant-free emulsion polymerisation reaction since surfactants provided negative effects to people and ecosystems [26]. Apart from that, this research also involved deionised water as a medium of reaction. On the other hand, Ag-Cu NPs was synthesised separately by chemical reduction with sodium borohydride. Notably, these Ag and Cu metals were rarely studied as compared to Au as these particular metals have complex LSPR in which both oscillated at short and long axes [12]. Furthermore, this synthesised 3D-MDPCs have the potency to be applied as substrate on SERS instrument to determine the fingerprint of a molecule structure in chemistry.

## EXPERIMENTAL

### Chemicals and Materials

For the synthesis of styrene methyl methacrylate copolymer (SMMA), all the chemical and standard supplies used were bought from Sigma Aldrich Company and R&D marketing. The chemicals were methyl methacrylate monomer (MMA), styrene monomer (STY), sodium hydroxide (NaOH), potassium persulphate (KPS), ammonium hydroxide (NH<sub>4</sub>OH), hydrogen peroxide (H<sub>2</sub>O<sub>2</sub>) and deionised water (dH<sub>2</sub>O) with a resistivity of 18.0MΩ. In the synthesis of bimetallic Ag-Cu alloy NPs, the chemicals used were silver nitrate (AgNO<sub>3</sub>), copper chloride (CuCl<sub>2</sub>), sodium borohydride (NaBH<sub>4</sub>), ethanol, deionised water (dH<sub>2</sub>O) and calcium chloride (CaCl<sub>2</sub>) for drying in the desiccator. For the preparation of SMMA@Ag-Cu core shell, polyethylene imine (PEI) was used as a linker to correlate between copolymer and alloy.

### Synthesis of Styrene Methyl Methacrylate Copolymer (SMMA)

Synthesis of SMMA was carried out via surfactant free emulsion copolymerisation and varied in MMA: STY ratio. In a fume hood, a reflux condenser was connected with 250 ml tri-neck round bottom flask equipped with magnetic stirrer and poured with 100 ml of deionised water. The system was heated to 70 °C

through silicon oil bath while purging with nitrogen gas (N<sub>2</sub>) and stirred at 350 rpm. These parameters were applied throughout the reaction. Once all the parameters remained constant, mixture of monomer MMA:STY was added into the flask followed by KPS initiator. After 8 h of reaction, the product was filtered by using a filter paper and centrifuged at 20,000 rpm by Eppendorf 5810. The obtained samples were washed successively by using deionised water.

### Surface Modification of SMMA with PEI

The dilution of PEI solution was conducted for 100 ml by mixing 2.8 ml of PEI with deionised water. Then, 5 ml of prepared SMMA copolymer was mixed with diluted PEI solution. The mixture was then added into a beaker containing 100 ml of deionised water while stirring vigorously at 650 rpm. The reaction was left to stir for one day and the obtained SMMA-PEI suspension was centrifuged, redispersed and reagitated for at least six times.

### Synthesis of Ag-Cu Alloy NPs

Bimetallic Ag-Cu alloy NPs were synthesised via the metallic salt reduction method. Firstly, a round bottom flask wrapped with aluminium foil was purged with N<sub>2</sub> gas for a few minutes. Then, a mixture containing 10 ml of 0.1 mol AgNO<sub>3</sub> and 10 ml of 0.1 mol CuCl<sub>2</sub> was added into the flask and stirred with the aid of a magnetic stirrer for 10 min. Next, 0.3 mol of NaBH<sub>4</sub> solution was added gradually into the flask. After one h, the product was filtered and the precipitate was washed with ethanol in an ice-cold atmosphere. At the end of reaction, the green precipitate was filtrated and washed with ethanol. The following samples were dried in a desiccator having CaCl<sub>2</sub> at room temperature.

### Synthesis of SMMA@Ag-Cu Core Shell

Initially, the Ag-Cu NPs were diluted for 10 ml by mixing 0.02 g of solid alloy with deionised water. The reaction was further left to sonicate for at least one h to obtain a dark green solution. Then, 7.5 ml of SMMA-PEI was added to the prepared alloy solution. The SMMA was introduced dropwise at approximately 10 drops/min while continuously stirring at 400 rpm. After that, the reaction was left to stir for two days. The resulting pale blue solution of SMMA@Ag-Cu core-shell was centrifuged, redispersed and reagitated several times. The synthesised solid SMMA@Ag-Cu was further characterised to study their chemical properties.

### Fourier-Transform Infrared Spectroscopy (FTIR) Analysis

In this research, FTIR spectroscopy was used to study the functional groups present in SMMA, also to analyse copolymerisation of STY and MMA successiveness. FTIR spectra were recorded on a Perkin-Elmer 2000

FTIR spectroscopy. During the sample preparation, SMMA suspension was oven dried and the powder was pelleted with potassium bromide (KBr), whereas STY and MMA solution were dropped directly on sodium chloride (NaCl) disc. The analysis was performed at a range from  $4000\text{ cm}^{-1}$  to  $650\text{ cm}^{-1}$ .

### Scanning Electron Microscope (SEM)

The morphology of SMMA, Ag-Cu bimetallic alloy nanoparticles and SMMA@Ag-Cu core-shell were observed through scanning electron microscopy (SEM). For sample preparation, a few drops of diluted SMMA or SMMA@Ag-Cu suspension were placed on SEM sample stub and oven dried at  $60\text{ }^{\circ}\text{C}$  while  $0.05\text{ g}$  of Ag-Cu powder was placed directly on SEM sample stub. All samples were sputtered coat with gold before viewing to avoid charging effect from the electron bombardment. Samples of thin films were also sputtered coat with gold before viewing.

### Ultraviolet Spectroscopy (UV-Vis) Analysis

The optical activities study for Ag-Cu bimetallic alloy NPs and SMMA@Ag-Cu core shell was investigated via UV-vis spectroscopy to study the photonic and SPR properties, respectively. For sample preparation of Ag-Cu bimetallic alloy nanoparticles,  $0.02\text{ g}$  of Ag-Cu alloy was diluted with  $10\text{ ml}$  of deionised water and left to sonicate for at least one h before analysis, while SMMA@Ag-Cu suspension was analysed without any dilution.

### X-ray Diffraction Spectroscopy (XRD) Analysis

XRD is an effective scientific method for measuring the characteristics and behaviour of crystallinity and for estimating the crystal size of alloy nanoparticles. XRD was used to study the crystallinity and purity of the samples. The analysis was performed by using

fabricated Ag-Cu alloy NPs and SMMA@Ag-Cu thin film that was cut into  $2\text{ cm} \times 2\text{ cm}$  and the  $2\theta$  angle was set from  $10^{\circ}$  to  $85^{\circ}$ .

### Electron Dispersion X-ray Spectroscopy (EDX) Analysis

Elemental analysis study for SMMA copolymer, Ag-Cu NPs and SMMA@Ag-Cu core shell was performed via energy dispersive X-Ray spectroscopy (EDX) analysis. The mapping was performed at a few different spots with  $10,000$  magnifications, spot size of  $6\text{ mm} \times 5\text{ mm}$  and  $10\text{ mm}$  working distance.

### Transmittance Electron Microscope (TEM) Analysis

The morphology of SMMA@Ag-Cu core-shell was also observed through TEM. For TEM sample preparation, dispersed SMMA@Ag-Cu core-shell suspension was dropped onto a copper grid and left for  $10\text{ min}$ . The excess sample was removed by using clean tissue papers and carefully transferred onto the sample holder prior to analysis.

## RESULTS AND DISCUSSION

### Synthesis of SMMA Copolymer

Physically STY and MMA monomer are colourless liquids, but synthesised SMMA copolymer appeared as milky white suspension. Even though, the colour changes were noticed during the synthesis, the successiveness of SMMA copolymerisation was analysed via FTIR spectroscopy by investigating the functional group present in synthesised SMMA copolymers. Based on the FTIR spectroscopy shown in Figure 1, the functional group existed in SMMA copolymer, especially the carbonyl group (C=O) bond and (C-H) benzene bond revealed in the spectra.

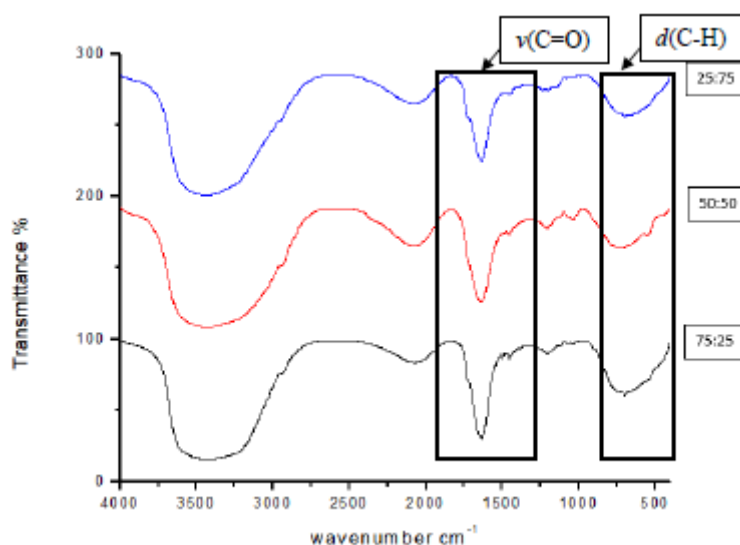


Figure 1. FTIR spectra of SMMA copolymer.

Sharp peak was observed around  $1670\text{ cm}^{-1}$  for the three ratios, indicating the existence of C=O functional group and a medium peak at  $760\text{ cm}^{-1}$  indicating the presence of aromatic C-H functional group. However, a broad peak of O-H stretches approximately  $3480\text{ cm}^{-1}$  appeared in the FTIR spectra of SMMA copolymer indicating the presence of water vapour in the sample. This error may be due to the incomplete drying of solvent during sample preparation part for FTIR analysis.

The morphology and structure for both 25:75 and

50:50 ratios of SMMA copolymers were studied by using SEM analysis. Based on SEM image shown in Figure 2, monodispersed, unaggregated and homogenous copolymer microspheres were successfully synthesised for both ratio of SMMA copolymers. Moreover, the SMMA copolymer spheres were packed together and formed a well-ordered arrangement of colloidal crystals. However, in terms of particle size analysis by using SEM measuring tools, it showed that the ratio of 50:50 SMMA was smaller in the size of polymer spheres as compared to a ratio of 25:75 SMMA (Table 1).

**Table 1.** Particle size of synthesised SMMA.

MMA:STY	Particle size (nm)
25:75	440
50:50	402

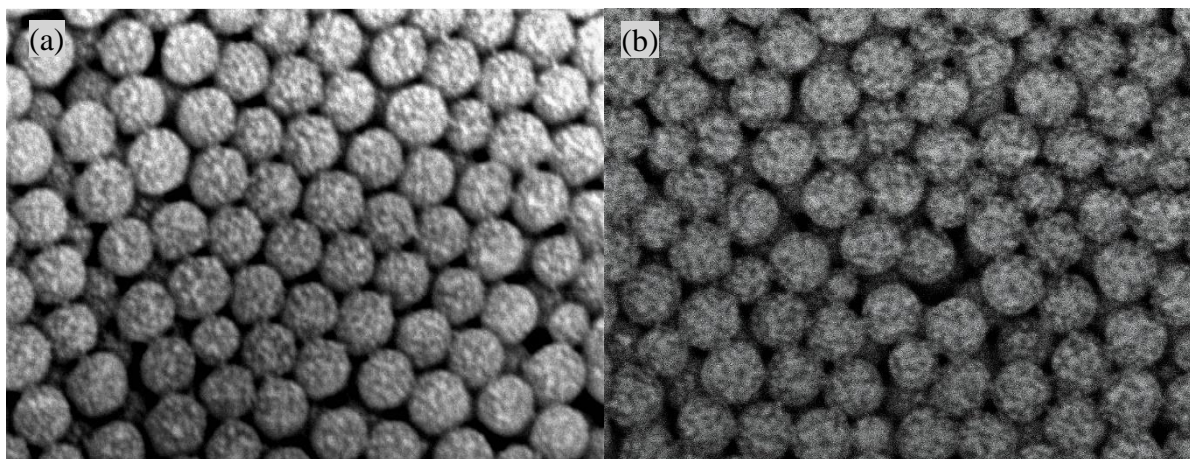


**Figure 2.** SEM image of SMMA copolymer of (a) 25:75 ratio (b) 50:50 ratio.

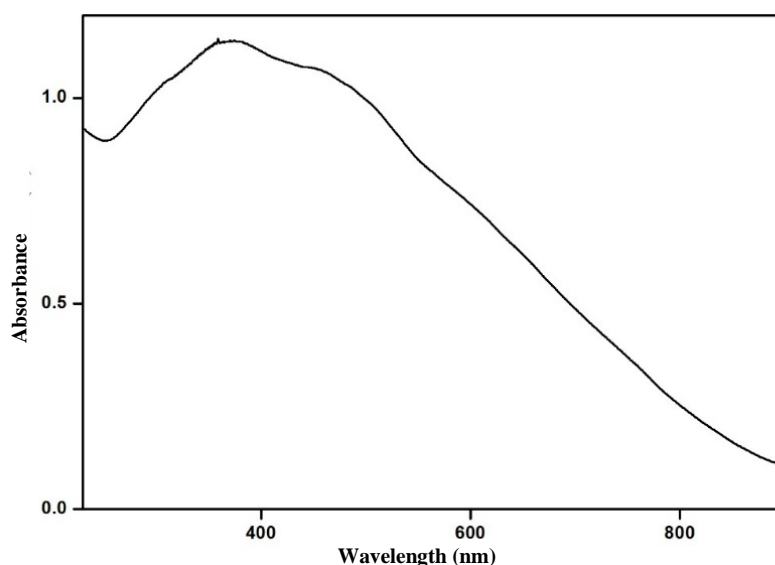


**Figure 3.** UV-vis spectrum of Ag-Cu bimetallic alloy NPs.

### Synthesis of Ag-Cu Bimetallic Alloy NPs

Bimetallic Ag-Cu alloy NPs synthesised via metallic salt reduction method emerged as green powder. In this part, UV-vis analysis is one of the most important explorations since it determines the intensity of absorption of the alloy NPs. Based on the UV-vis spectrum in Figure 3 showed a strong absorption peak at 380 nm in near visible region of electromagnetic spectrum. Additionally, the formation of a single peak proved that the combination of Ag and Cu to form bimetallic alloy NPs was successful. This is because, pure Ag and Cu showed a strong absorption peak at 431 nm and 592 nm, respectively [27].

In addition, SEM analysis was also conducted to determine the size and morphology of synthesised Ag-Cu alloy NPs represented in Figure 4. However, the structural and morphological analysis of Ag-Cu NPs could not be performed properly since it was

difficult to capture the sharp SEM image of Ag-Cu NPs. However, based on the SEM images shown in Figure 4, it can be concluded that the Ag-Cu bimetallic alloy NPs were successfully synthesised since they were in spherical shape and some of the particles were connected to each other. On this point, the particles that linked to each other were considered as alloys [28].

Besides, XRD analysis was also conducted to study the crystallinity of Ag-Cu NPs. Figure 5 represents the experimental XRD pattern of Ag-Cu alloy synthesised from the chemical reduction of  $\text{AgNO}_3 + \text{CuCl}_2$  and compared with the XRD spectrum in previous literature. From the spectrum, four intense peaks were identified at position  $2\theta$  of  $37.8^\circ$ ,  $44.1^\circ$ ,  $64.2^\circ$  and  $77.24^\circ$ . The peaks at  $37.8^\circ$  attributed to the formation of Ag-Cu alloy nanoparticles, whereas other peaks at  $44.1^\circ$ ,  $64.2^\circ$  and  $77.24^\circ$  showed a less intense in the XRD spectrum,

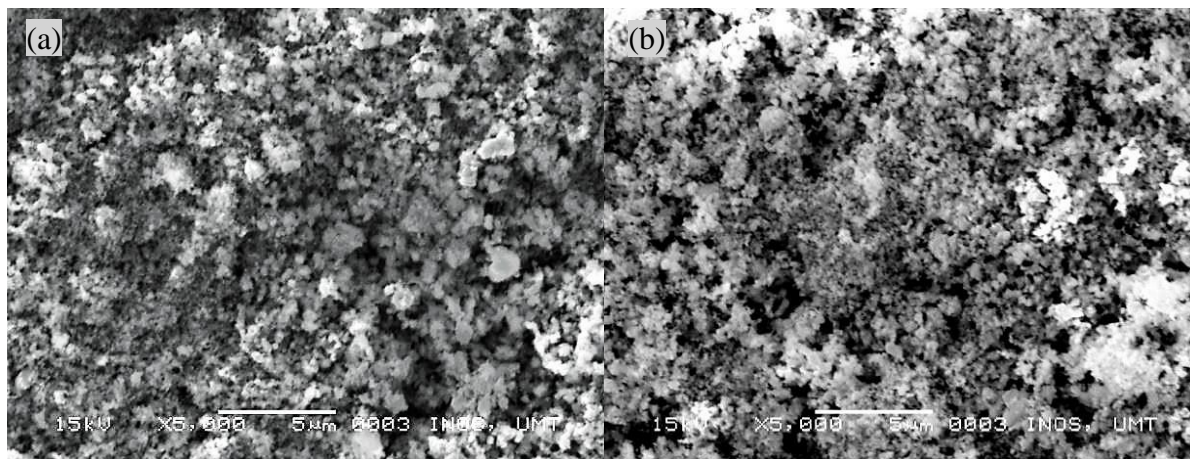


Figure 4. SEM image of Ag-Cu alloy NPs (a) without gold coating (b) with gold coating.

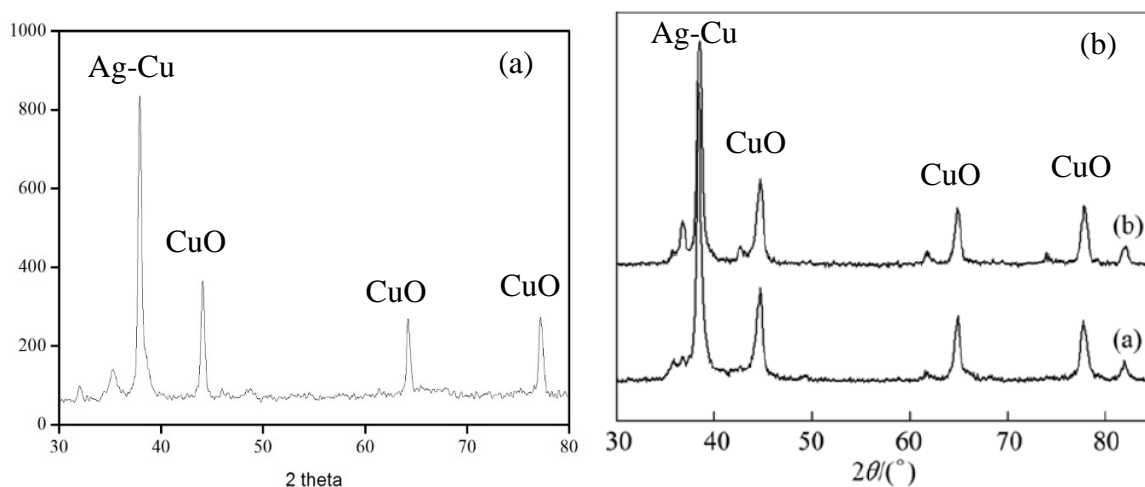


Figure 5. (a) XRD spectrum of synthesized Ag-Cu alloy NPs and (b) XRD spectrum of Ag-Cu alloy NPs in previous literature [29].

indicating the presence of copper oxide (CuO) in samples [29]. The appearance of CuO may be due to the oxidation of copper in samples during sample preparation. Therefore, XRD characterisation proved the successful formation of Ag-Cu alloy NPs instead of the mixture of Ag and Cu.

Additionally, EDX analysis was also performed to determine the percentage of each element presence in the sample. Based on the EDX spectrum shown in Figure 6, each element represented in Ag-Cu alloy

NPs was shown successfully. However, the presence of oxygen may be due to the oxidation of some Cu metals to form CuO during the synthesis. Table 2 indicates the interpretation of EDX spectrum where the percentage amount of oxygen was 0.67 %, while for Ag and Cu the percentage amount were 34.35% and 65.31%, respectively. These indicated that the sample was an alloy of Ag-Cu instead of individual Ag and Cu. In addition, the percentage amount of oxygen proved that the sample did not undergo complete oxidation.

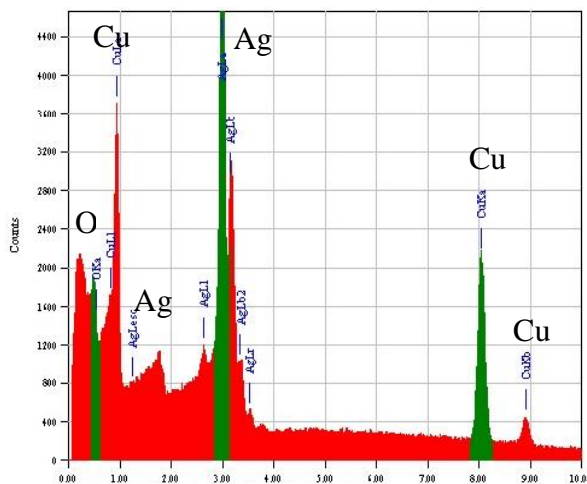


Figure 6. EDX spectrum of Ag-Cu NPs.

Table 2. EDX analysis of Ag-Cu NPs.

Elements	Mass Percentage (%)	Weight Percentage (%)
Ag	0.17	34.35
Cu	0.66	65.31
O	0.09	0.67

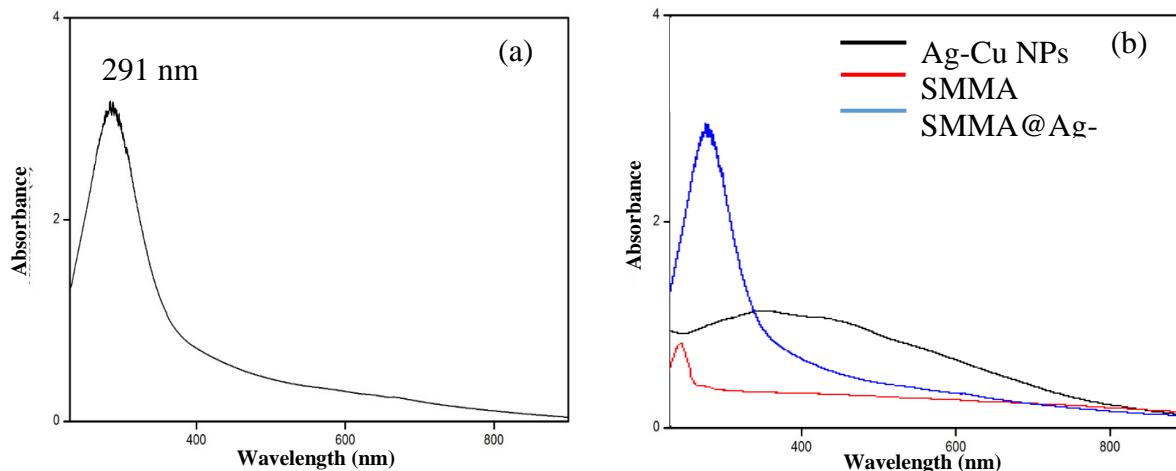


Figure 7. UV-vis absorbance of (a) SMMA@Ag-Cu alloy core-shell (b) Overlapped SMMA copolymer, Ag-Cu alloy and SMMA@Ag-Cu core shell.

### Synthesis of SMMA@Ag-Cu Core Shell

The synthesised SMMA@Ag-Cu core shell was in a light blue solution. In order to study the interaction of the core shell with light, UV-vis analysis was conducted on synthesised MDPCs. Figure 7(a) shows a sharp peak obtained at 291 nm that slightly shifted to the left as compared to Ag-Cu UV-vis analysis and shifted to the right as compared to SMMA copolymer UV-vis analysis shown in Figure 3. This is because, it was acknowledged that the combination of copolymer and metal NPs had improved the mechanical and electrical properties of photonic crystals [30]. Therefore, the UV-vis analysis of SMMA@Ag-Cu indicated that the resulting core-shell structure had improved the absorbance efficiency as compared to alloy and copolymer alone. Also, it directly deduced that the combination of copolymer and alloy NPs was successful, as well enhanced the absorbance efficiency.

Furthermore, TEM characterisation was conducted on SMMA@Ag-Cu core-shell to study the morphological and structural behaviour of the core shell. Based on the TEM image in shown Figure 8, SMMA copolymer nano spheres could be observed with average sizes of 450 nm and were also clustered together owing to the strong attraction effects of the PEI linker. Unfortunately, the presence of Ag-Cu alloy NPs was incapable to be observed in TEM analysis. The Ag-Cu bimetallic alloy NPs was complicated to be analysed using microscopic imaging since highly distributed metal species may be mobile, even at room temperature, depending on the surrounding gas particles [31].

### CONCLUSION

In conclusion, SMMA@Ag-Cu a metallo-dielectric photonic crystal (MDPC) was successfully produced by using SMMA photonic crystal as building block,

while Ag-Cu bimetallic alloy nanoparticles as the metallic core shell. Significantly, a green chemistry approach has been taken for the synthesis of mono-dispersed SMMA copolymer, whereby surfactant free emulsion copolymerisation reaction was employed and deionised water, a non-toxic solvent was used as a medium throughout the synthesis. Optically active and stable Ag-Cu alloy NPs synthesised from the chemical reduction method produced a high yield of alloy combination instead of individual Ag and Cu metals.

Moreover, the SMMA@Ag-Cu also had unique optical properties, such as high dielectric constant and produced higher absorbance in UV-vis analysis as compared to Ag-Cu alloy and SMMA alone. In this context, it was proven that the invention of replacing a single polymer with SMMA copolymer elevated the heat resistance and was able to be fabricated as SERS substrate since it was capable to endure several Raman lasers [32]. Likewise, a substrate incorporated by using Ag merged with Cu could also promote SERS activity when detailed control in their compositions was applied [12]. Even though, the UV-vis results showed that SMMA@Ag-Cu had plasmonic properties. Further control over particle size, density and the surrounding medium's dielectric properties is still required to improve the electromagnetic properties on the surface for SERS activity [33]. Hence, this SMMA@Ag-Cu MDPC also has the potential to be used in various applications, especially as SERS substrate.

### ACKNOWLEDGEMENTS

The authors would like to thank the Ministry of Education of Malaysia for Fundamental Research Grant Scheme (FRGS) 59630 (FRGS/1/2020/STG05/UMT/02/4) and Universiti Malaysia Terengganu for funding this research. We also would like to acknowledge all persons, authorities and institutions involved to make this research successful.

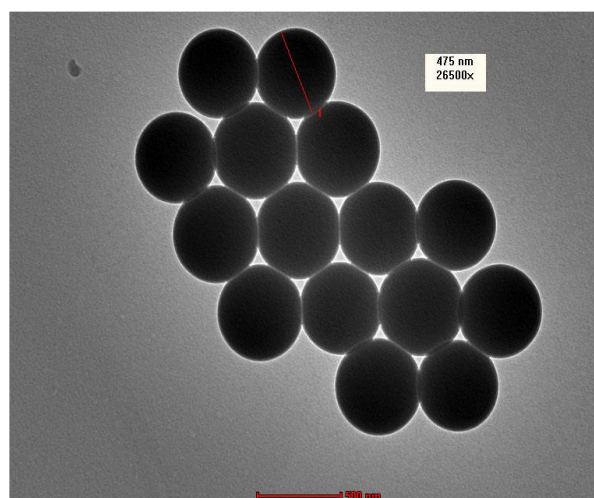


Figure 8. TEM images of SMMA@Ag-Cu core shell.

## REFERENCES

1. Yablonovitch, E. (1987) Inhibited Spontaneous Emission in Solid-State Physics and Electronics. *Physical Review Letters*, **58**, 2059–2062. doi: 10.1103/physrevlett.58.2059.
2. Al-Azawi, M. A., Bidin, N., Bououdina, M. & Mohammad, S. M. (2016) Preparation of gold and gold–silver alloy nanoparticles for enhancement of plasmonic dye-sensitized solar cells performance. *Solar Energy*, **126**, 93–104. <https://doi.org/10.1016/j.solener.2015.12.043>.
3. Ahmad, H., Tahrin, R. A. A., Azman, N., Kassim, S., Ismail, M. A. & Maah, M. J. (2017) 1.5-micron fiber laser passively mode-locked by gold nano-particles saturable absorber. *Optics Communications*, **403**, 115–120. <https://doi.org/10.1016/j.optcom.2017.06.094>.
4. Colusso, E., De Ferrari, F., Minzioni, P., Martucci, A., Wang, Y. & Omenetto, F. G. (2018) Engineering optical defects in biopolymer photonic lattices. *Journal of Materials Chemistry C*, **6(5)**, 966–971. <https://doi.org/10.1039/c7tc04404f>.
5. Bockstaller, M., Kolb, R. & Thomas, E. L. (2001) Metallodielectric Photonic Crystals Based on Diblock Copolymers. *Advanced Materials*, **13(23)**, 1783–1786. [https://doi.org/10.1002/15214095\(200112\)13:23<1783::aid-adma1783>3.0.co;2-x](https://doi.org/10.1002/15214095(200112)13:23<1783::aid-adma1783>3.0.co;2-x).
6. Saurav, K., Kumari, S. & Le Thomas, N. (2017) CMOS Fabricated Large Array of Free Standing Substrate-Less Photonic Crystal Cavities for Biosensing Applications. *IEEE Photonics Journal*, **9(2)**, 1–8. <https://doi.org/10.1109/jphot.2017.2684627>.
7. Khan, M. U., McGrath, J., Corbett, B. & Pemble, M. (2017) Air-clad broadband waveguide using micro-molded polyimide combined with a robust, silica-based inverted opal substrate. *Optical Materials Express*, **7(9)**, 3155. <https://doi.org/10.1364/ome.7.003155>.
8. Altunbek, M., Kuku, G. & Culha, M. (2016) Gold Nanoparticles in Single-Cell Analysis for Surface Enhanced Raman Scattering. *Molecules*, **21(12)**, 1617. <https://doi.org/10.3390/molecules21121617>.
9. Khairunisa, W. N. (2016) Synthesis and Characterization of polystyrene via emulsion polymerization based on Photonic Crystals. *Bcs. Thesis*.
10. Fudouzi, H. (2004) Fabricating high-quality opal films with uniform structure over a large area. *Journal of Colloid and Interface Science*, **275(1)**, 277–283. <https://doi.org/10.1016/j.jcis.2004.01.054>.
11. Zhang, X., Gao, J., Hong, C., Han, J. & Han, W. (2013) Observation of SiC nanodots and nano-wires in situ growth in SiOC ceramics. *CrystEngComm*, **15(38)**, 7803. <https://doi.org/10.1039/c3ce40924d>.
12. He, L., Liu, C., Tang, J., Zhou, Y., Yang, H., Liu, R. & Hu, J. (2018) Self-catalytic stabilized Ag-Cu nanoparticles with tailored SERS response for plasmonic photocatalysis. *Applied Surface Science*, **434**, 265–272.
13. Han, Q., Zhang, C., Gao, W., Han, Z., Liu, T., Li, C., Wang, Z., He, E. & Zheng, H. (2016) Ag-Au alloy nanoparticles: Synthesis and in situ monitoring SERS of plasmonic catalysis. *Sensors and Actuators B: Chemical*, **231**, 609–614. <https://doi.org/10.1016/j.snb.2016.03.068>.
14. Van, X. T., Trinh, L. T., Van Pham, H. & Nguyen, M. T. T. (2022) Tunable Plasmonic Properties of Bimetallic Au-Cu Nanorods for SERS-Based Sensing Application. *Journal of Electronic Materials*, **51(4)**, 1857–1865. <https://doi.org/10.1007/s11664-022-09455-4>.
15. Wang, Z. -J., Wang, X., Lv, J. -J., Feng, J. -J., Xu, X., Wang, A. -J. & Liang, Z. (2017) Bimetallic Au-Pd nanochain networks: facile synthesis and promising application in biaryl synthesis. *New Journal of Chemistry*, **41(10)**, 3894–3899. <https://doi.org/10.1039/c7nj00998d>.
16. Toshima, N. & Yonezawa, T. (1998) Bimetallic nanoparticles—novel materials for chemical and physical applications. *New Journal of Chemistry*, **22(11)**, 1179–1201. <https://doi.org/10.1039/a805753b>.
17. Monga, A. & Pal, B. (2015) Improved catalytic activity and surface electro-kinetics of bimetallic Au–Ag core–shell nanocomposites. *New Journal of Chemistry*, **39(1)**, 304–313. <https://doi.org/10.1039/c4nj01419g>.
18. Fernández-Navarro, C., Mejía-Rosales, S. & Tlahuice-Flores, A. (2018) Structural Diagram of  $AuCu_{1-x}$  Nanoparticles: Dependency of Geometry on Composition and Size. *Journal of Cluster Science*, **29(4)**, 815–823. <https://doi.org/10.1007/s10876-018-1399-x>.
19. Bakina, O., Glazkova, E., Pervikov, A., Lozhkomoev, A., Rodkevich, N., Svarovskaya, N., Lerner, M.,

- 259 Wan Ahmad Lutfil Hadi Wan Abdul Halim, Nor Shafeera Rasyada Shaiful Bahri, Nur Aida Mohamed Shaul Hamid and Syara Kassim
- Naumova, L., Varnakova, E. & Chjou, V. (2020) Design and Preparation of Silver–Copper Nanoparticles for Antibacterial Applications. *Journal of Cluster Science*, **32**(3), 779–786. <https://doi.org/10.1007/s10876-020-01844-1>.
20. Tsai, C. -H., Chen, S. -Y., Song, J. -M., Chen, I. -G. & Lee, H. -Y. (2013) Thermal stability of Cu@Ag core–shell nanoparticles. *Corrosion Science*, **74**, 123–129. <https://doi.org/10.1016/j.corsci.2013.04.032>.
21. Chen, K., Ray, D., Peng, Y. & Hsu, Y. -C. (2013) Preparation of Cu–Ag core–shell particles with their anti-oxidation and antibacterial properties. *Current Applied Physics*, **13**(7), 1496–1501. <https://doi.org/10.1016/j.cap.2013.05.003>.
22. Rao, V. K., Ghildiyal, P. & Radhakrishnan, T. P. (2017) In Situ Fabricated Cu–Ag Nanoparticle-Embedded Polymer Thin Film as an Efficient Broad Spectrum SERS Substrate. *The Journal of Physical Chemistry C*, **121**(2), 1339–1348. <https://doi.org/10.1021/acs.jpcc.6b10238>.
23. Bao, G., Xu, Y., Huang, L., Lu, X., Zhang, L., Fang, Y., Meng, L. & Liu, J. (2015) Strengthening Effect of Ag Precipitates in Cu–Ag Alloys: A Quantitative Approach. *Materials Research Letters*, **4**(1), 37–42. <https://doi.org/10.1080/21663831.2015.1091795>.
24. Rtimi, S., Sanjines, R., Pulgarin, C. & Kiwi, J. (2015) Microstructure of Cu–Ag Uniform Nanoparticulate Films on Polyurethane 3D Catheters: Surface Properties. *ACS Applied Materials & Interfaces*, **8**(1), 56–63. <https://doi.org/10.1021/acsami.5b09738>.
25. Chen, K., Zhang, X., Zhang, Y., Lei, D. Y., Li, H., Williams, T. & MacFarlane, D. R. (2016) Highly Ordered Ag/Cu Hybrid Nanostructure Arrays for Ultrasensitive Surface-Enhanced Raman Spectroscopy. *Advanced Materials Interfaces*, **3**(13), 1600115. <https://doi.org/10.1002/admi.201600115>.
- Synthesis of Bimetallic Silver and Copper Alloy Nanoparticles Embedded with Styrene-Methyl Methacrylate Copolymer Nanosphere (SMMA@Ag-Cu) as a Potential Surface Enhanced Raman Scattering (SERS) Substrate
26. Badmus, S. O., Amusa, H. K., Oyehan, T. A. & Saleh, T. A. (2021) Environmental risks and toxicity of surfactants: overview of analysis, assessment, and remediation techniques. *Environmental Science and Pollution Research*. <https://doi.org/10.1007/s11356-021-16483-w>.
27. Nanda, K. K. (2009) Size-dependant melting of nanoparticles: Hundred Years of thermodynamic model. *Pramana Journal of Physics*, **72**(4), 617–628.
28. Gong, C. & Leite, M. S. (2016) Noble Metal Alloys for Plasmonics. *ACS Photonics*, **3**(4), 507–513. <https://doi.org/10.1021/acsp Photonics.5b00586>.
29. Bhagathsingh, W. & Nesaraj, A. S. (2013) Low temperature synthesis and thermal properties of Ag–Cu alloy nanoparticles. *Transactions of Non-ferrous Metals Society of China*, **23**(1), 128–133. [https://doi.org/10.1016/s1003-6326\(13\)62438-3](https://doi.org/10.1016/s1003-6326(13)62438-3).
30. Alhusaiki-Alghamdi, H. M. (2019) Improve spectroscopic structural and AC electrical conductivity of PC/PEO blend using graphene. *Results in Physics*, **12**, 793–798 (October 2018).
31. Smith, D. J. (2015) Chapter 1. characterization of nanomaterials using transmission electron microscopy. *Nanoscience & Nanotechnology Series*, 1–29. <https://doi.org/10.1039/9781782621867-00001>.
32. Kassim, S., Mukhtar, N. A. & Tahrin, R. A. A. (2020) Synthesis and Characterization of Plasmon-Enhanced SERS Substrate Based on Au-Ag Alloy-Coated, Large-Area Photonic (Methyl Methacrylate+ Styrene) Co-Polymer. *Materials Science Forum*, **982**, 14–19. <https://doi.org/10.4028/www.scientific.net/msf.982.14>.
33. Zhao, Y., Zhang, X. -J., Ye, J., Chen, L. -M., Lau, S. -P., Zhang, W. -J. & Lee, S. -T. (2011) Metallo-Dielectric Photonic Crystals for Surface-Enhanced Raman Scattering. *ACS Nano*, **5**(4), 3027–3033. <https://doi.org/10.1021/nn2001068>.